

## RESEARCH LETTER

10.1002/2015GL065959

## Key Points:

- Production rates of in situ cosmogenic isotopes are used for paleoelevation
- Uplift of the Andes by mantle delamination in the late Miocene is ruled out
- The Precordillera attained a substantial part of its elevation by 14 Ma

## Supporting Information:

- Supporting Information S1

## Correspondence to:

L. A. Evenstar,  
levenstar@bristol.ac.uk

## Citation:

Evenstar, L. A., F. M. Stuart, A. J. Hartley, and B. Tattitch (2015), Slow Cenozoic uplift of the western Andean Cordillera indicated by cosmogenic  $^3\text{He}$  in alluvial boulders from the Pacific Planation Surface, *Geophys. Res. Lett.*, 42, 8448–8455, doi:10.1002/2015GL065959.

Received 31 AUG 2015

Accepted 8 OCT 2015

Accepted article online 12 OCT 2015

Published online 29 OCT 2015

Corrected 5 JAN 2016

This article was corrected on 5 DEC 2015. See the end of the full text for details.

©2016. The Authors.

This is an open access article under the terms of the Creative Commons Attribution License, which permits use, distribution and reproduction in any medium, provided the original work is properly cited.

## Slow Cenozoic uplift of the western Andean Cordillera indicated by cosmogenic $^3\text{He}$ in alluvial boulders from the Pacific Planation Surface

Laura A. Evenstar<sup>1</sup>, Finlay M. Stuart<sup>2</sup>, Adrian J. Hartley<sup>3</sup>, and Brian Tattitch<sup>1</sup>

<sup>1</sup>School of Earth Science, University of Bristol, Bristol, UK, <sup>2</sup>Isotope Geoscience Unit, Scottish Universities Environmental Research Centre, Glasgow, UK, <sup>3</sup>Department of Geology and Petroleum Geology, University of Aberdeen, Aberdeen, UK

**Abstract** To determine the mechanisms responsible for mountain belt growth, it is important to accurately establish the timing of surface uplift. Here we exploit the altitude control on the production rate of in situ cosmogenic nuclides to test the hypothesis that the Andes was uplifted in the late Miocene. High concentrations of in situ cosmogenic  $^3\text{He}$  ( $^3\text{He}_{\text{cos}}$ ) have previously been measured in alluvial boulders on the western flank of the Central Andes, northern Chile (Evenstar et al. 2009). These are consistent with deposition soon after formation of the surface (13–14 Ma). We have modeled the accumulation of cosmogenic  $^3\text{He}$  in several different surface uplift scenarios and compared them to the measured concentrations. The measured  $^3\text{He}_{\text{cos}}$  concentrations are too high to be produced by late Miocene uplift and imply that the western flank of the Andean Cordillera attained a substantial part of its current elevation prior to 14 Myr ago.

### 1. Introduction

The elevation history of mountain belts such as the Himalayas, North American Rockies, Andes, and Alps have been used to explain continental tectonic processes, orogenic erosion, and changes to the global climate [e.g., Clift, 2010]. However, there is typically a significant uncertainty associated with the timing and magnitude of surface uplift that has led to a wide range of mechanisms to account for orogenic uplift.

The lack of unequivocal constraints on the mean elevation history of the Central Andes has led to competing theories to account for the generation of the mountain belt. These hypotheses have been simplified into two general scenarios by Barnes and Ehlers [2009]: (i) late Miocene uplift, where surface uplift of ~2.5 km occurred between 11 and 6 Ma [Fariás et al., 2005; Garzzone et al., 2006; Ghosh et al., 2006; Molnar and Garzzone, 2007; Garzzone et al., 2008; Hoke and Garzzone, 2008] due to large-scale mantle delamination and (ii) early Miocene (or earlier) uplift, where gradual surface uplift initiated in the late Eocene is associated with crustal shortening and thickening in response to oblique subduction of the Nazca plate [e.g., Victor et al., 2004; Barke and Lamb, 2006; Hartley et al., 2007; Barnes and Ehlers, 2009].

The evidence for late Miocene uplift is based on a number of studies that have utilized climate sensitive-altitude relationships, such as oxygen isotopes [Garzzone et al., 2006], clumped C-O isotopes [Ghosh et al., 2006; Quade et al., 2007], and fluvial incision rate [Schildgen et al., 2007; Hoke et al., 2007; Thouret et al., 2007]. The isotope-based techniques assume that the present-day relationship between meteoritic water, surface temperatures, and elevation can be used to reconstruct past elevations which suggest that the majority of uplift occurred after 10 Ma. However, there are a number of uncertainties associated with this technique [Hartley et al., 2007; Ehlers and Poulsen, 2009; Jeffery et al., 2013]. Recent modeling of climate change associated with Andean uplift shows that this overestimates uplift rates, as precipitation levels, surface temperature, and wind direction have varied during uplift [Ehlers and Poulsen, 2009]. It also predicts an increase in precipitation along the Western Cordillera that would account for the rapid fluvial incision, rather than resulting from surface uplift [Jeffery et al., 2013]. A recent reassessment suggests that the existing data cannot distinguish between late Miocene or early Miocene (or earlier) uplift histories leading to an array of competing theories to account for the generation of the mountain belt [Barnes and Ehlers, 2009]. Without independent constraints on the timing and rate of surface uplift it is difficult to determine which tectonic processes are responsible for the formation of the Andean mountain belt.

The production rate of in situ cosmogenic nuclides at the Earth surface is strongly altitude dependent and where slowly eroding surfaces are preserved they have the potential to be used to decipher the surface uplift

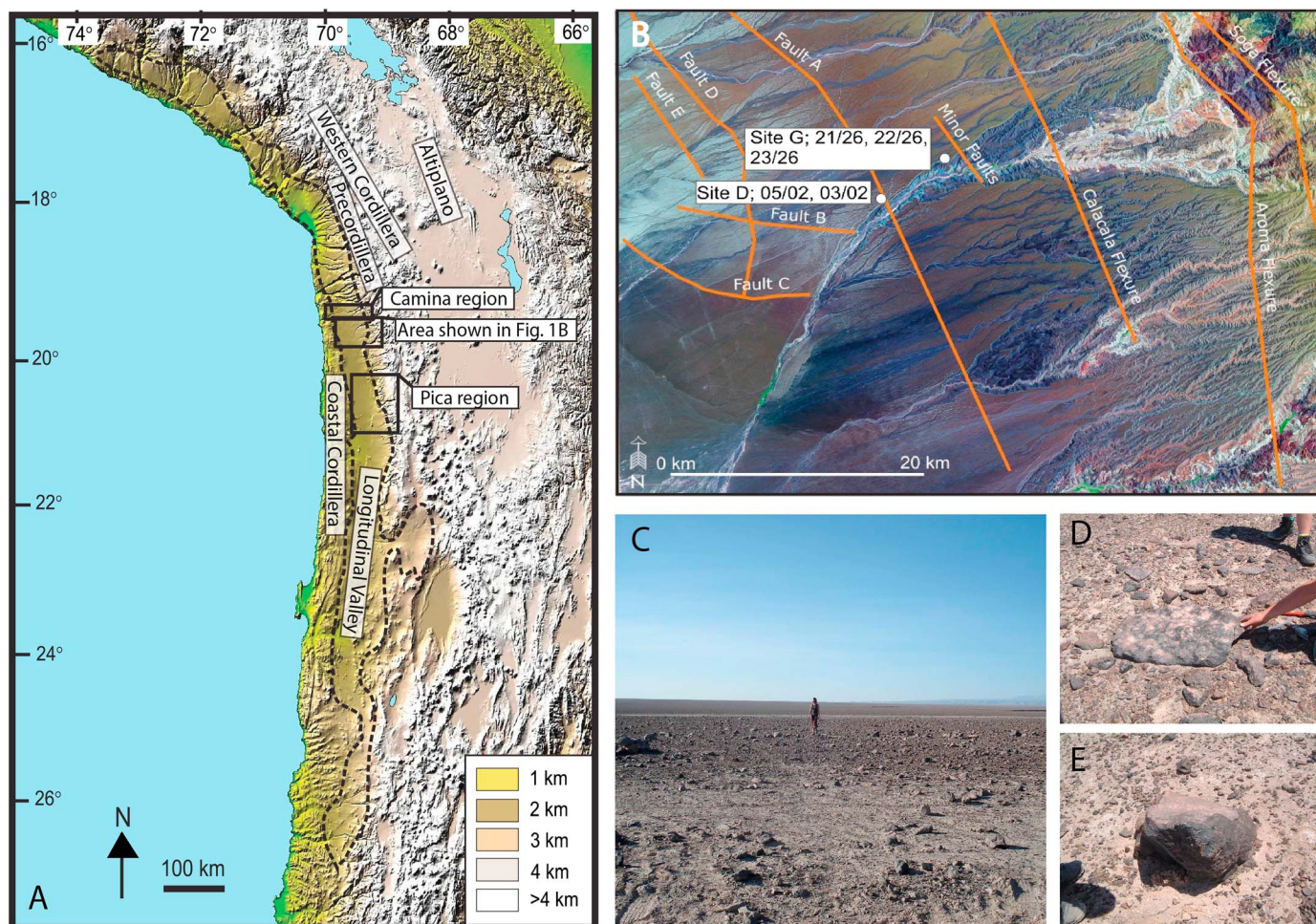


**Figure 1.** (a) Location of study area in the Atacama Desert (Digital Elevation Model (DEM) based on GTOPO30). The Pacific Planation Surface is located within the dashed line. Boxes show the location of the Aroma Quebrada and Pica region area studied by Victor *et al.* [2004]. (b) Landsat image of the Aroma Quebrada with location of samples. Soga Flexure, Aroma Flexure, and Calacala Flexure were mapped by Farias *et al.* [2005]. Faults A–E are identified from landsat images. (c) Photographs of the Pacific planation surface with rounded alluvial/fluvial boulders, (d) sample 03/02, and (e) sample 05/02.

history of mountain ranges that is independent of climate [e.g., Riihimaki and Libarkin, 2007]. The cosmogenic noble gas isotopes,  $^3\text{He}$  and  $^{21}\text{Ne}$ , are stable and are used to quantify rates of long-term landscape development [e.g., Margerison *et al.*, 2005]. The Atacama Desert is a natural laboratory for testing uplift histories using in situ cosmogenic nuclides. The extremely low erosion rates result in exceptionally high concentrations of cosmogenic noble gas isotopes in depositional features [Dunai *et al.*, 2005; Nishiizumi *et al.*, 2005; Kober *et al.*, 2006; Evenstar *et al.*, 2009], and precisely dated volcanic rocks allow constraints to be put on the absolute age of surfaces [Victor *et al.*, 2004; Muñoz and Sepúlveda, 1992].

Here we use the concentration of cosmogenic  $^3\text{He}$  in alluvial boulders from a slowly eroding Miocene-Pliocene-aged surface from the western flank of the Central Andes to test the hypothesis that the Andes mountain belt formed largely in the late Miocene. Unlike other approaches, this technique is not reliant on complex climate sensitive-altitude relationships and may have potential for application in other mountain belts.

## 2. Geological Background

The western side of the Central Andes can be divided into five different morphotectonic provinces. From west to east these are the Coastal Cordillera, Longitudinal Valley, Precordillera, Western Cordillera, and Altiplano. The Coastal Cordillera forms a coastal escarpment rising up from sea level to an average elevation of 1000 m. The Longitudinal Valley is a forearc basin filled by Eocene to Miocene sediments derived from the east [Hartley *et al.*, 2000; Pinto *et al.*, 2007]. Sedimentation ceased diachronously from middle Miocene to

**Table 1.** Concentration of <sup>3</sup>He in Alluvial Boulders From the Quebrada Aroma Region After *Evenstar et al.* [2009] Reduced to Account for <sup>3</sup>He Contribution From Neutron Capture on Li

Site	Altitude	Sample	<sup>3</sup> He (10 <sup>9</sup> atoms/g)
G	1900	21/26	3.03 ± 0.095
		22/26	3.04 ± 0.096
		23/26	3.87 ± 0.030
D	1690	03/02	2.54 ± 0.049
		05/02	2.64 ± 0.036

arc blanketed by early Miocene ignimbrite sheets [*Wörner et al.*, 2002]. To the east, the Western Cordillera is a 50 to 100 km wide modern magmatic arc. The Altiplano is a 200 km wide, internally drained basin at an average elevation of 3.8 km that lies east of the modern arc. The Coastal Cordillera, Longitudinal Valley, and part of the Precordillera form an area of extreme aridity due to combination of factors [*Hartley*, 2003]. The high aridity leads to some of the lowest erosion rates in the world and thus to some of the highest concentrations of in situ cosmogenic nuclides [*Dunai et al.*, 2005; *Kober et al.*, 2007; *Evenstar et al.*, 2009].

Two general models have been proposed to account for uplift within the Longitudinal Valley and Precordillera on the Western margin of the Andes supporting the end-member scenarios for Andean uplift. *Fariás et al.* [2005] and *Hoke et al.* [2007] presented evidence for significant uplift in the last 10 Myr. Both proposed that the PPS formed at ~10 Ma and suggested that significant incision into the paleosurface was initiated at 10 Ma due to regional tilting, isolating it from the Precordillera. In contrast, *Victor et al.* [2004] favored early Miocene (or earlier) surface uplift generated by movement along a series of reverse faults.

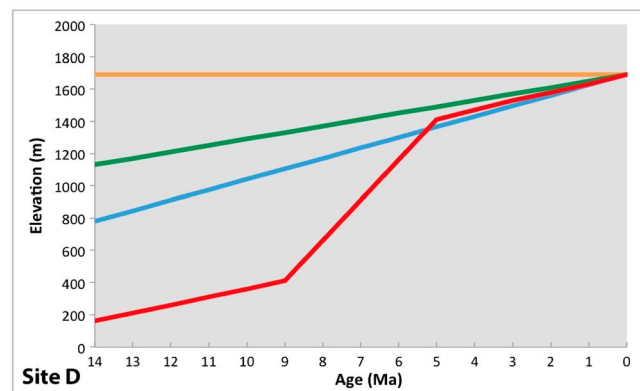
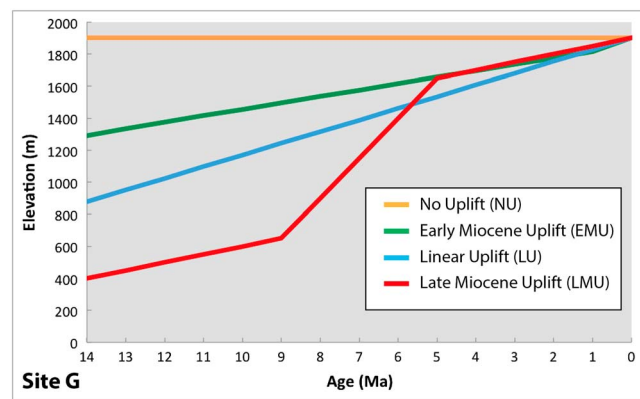


**Figure 2.** The paleoelevation histories since 14 Ma for site G (elevation 1900 m) and D (elevation 1690 m) used in this study. No uplift (NU), orange; early Miocene uplift (EMU), green; linear uplift (LU), blue; and late Miocene uplift (LMU), red.

middle Pliocene times, and a relict flat lying Pacific Planation Surface (PPS) developed [*Evenstar et al.*, 2009]. The PPS is 30 to 60 km wide with an average elevation of 1000 m. It slopes at 1.5–3° to the west from the Precordillera. The Precordillera ranges in elevation from 1000 to 4000 m and largely comprises the remnants of a late Cretaceous to Oligocene magmatic

These two surface uplift histories will produce significantly different cosmogenic nuclide concentrations in a non-eroding surface. Late Miocene uplift predicts that for a substantial part of the Miocene the paleosurface was at low elevation receiving lower cosmic ray flux for longer than if the main pulse of uplift had occurred in the early Miocene. By comparing the predicted concentration of <sup>3</sup>He with that measured in alluvial boulders that have been deposited on the paleosurface, we can test the timing and rate of uplift of the region.

### 3. In Situ Cosmogenic <sup>3</sup>He in Boulders From the Pacific Planation Surface

Cosmogenic <sup>3</sup>He concentrations are used from data published by *Evenstar et al.* [2009] on measured pyroxene and amphibole separated from 22 alluvial boulders of Miocene andesite that sit on the PPS in the Quebrada Aroma area, northern Chile (Figure 1). The boulders were selected on the basis of the absence of evidence of erosion and weathering. Five of the boulders (23/26, 21/26, 22/26, 03/02, and 05/02)

**Table 2.** Modeled Maximum <sup>3</sup>He Concentrations<sup>a</sup> Produced in Boulders From Quebrada Aroma, Northern Chile

Site	No Uplift			Early Miocene Uplift			Linear Uplift			Late Miocene Uplift		
	<i>Lal</i> [1991]	<i>Dunai</i> [2000]	<i>Lifton</i> et al. [2014]	<i>Lal</i> [1991]	<i>Dunai</i> [2000]	<i>Lifton</i> et al. [2014]	<i>Lal</i> [1991]	<i>Dunai</i> [2000]	<i>Lifton</i> et al. [2014]	<i>Lal</i> [1991]	<i>Dunai</i> [2000]	<i>Lifton</i> et al. [2014]
G	4.15 ± 0.11	3.76 ± 0.13	3.95 ± 0.12	3.43 ± 0.10	3.11 ± 0.09	3.25 ± 0.09	3.07 ± 0.08	2.80 ± 0.09	2.91 ± 0.08	2.78 ± 0.08	2.53 ± 0.08	2.58 ± 0.07
D	3.48 ± 0.08	3.16 ± 0.12	3.32 ± 0.10	2.94 ± 0.08	2.64 ± 0.08	2.80 ± 0.08	2.65 ± 0.07	2.42 ± 0.07	2.50 ± 0.08	2.30 ± 0.06	2.09 ± 0.06	2.12 ± 0.06

<sup>a</sup>All values are 10<sup>9</sup> atoms/g.

from two sites (D and G) have extremely high <sup>3</sup>He concentrations for their elevation (Table 1) that are broadly consistent with deposition at the time of, or soon after, formation of the paleosurface [Evenstar et al., 2009]. The PPS in Quebrada Aroma is developed on 300 m of alluvial gravels that originate from the Precordillera. The gravels overlie the 16.27 ± 0.16 Ma Nama ignimbrite (Member 4 of the Altos de Pica formation) [Pinto et al., 2004; Victor et al., 2004; Farías et al., 2005; Pinto et al., 2007]. Temporal constraints from dated volcanic rocks and magnetopolarity chronologies from the Camiña Valley, 25 km to the north of the Aroma Quebrada, show that 300 m of alluvium takes 3 to 5 Myr to accumulate [Pinto et al., 2004; von Rotz et al., 2005]. Using a conservative lower limit of 3 Myr for alluvium accumulation, the boulders overlying these sediments cannot have been exposed for more than 13.4 Myr.

#### 4. Uplift History Models

The measured cosmogenic <sup>3</sup>He in the five boulders is compared with concentrations produced in four different surface uplift models for the western flank of the Central Andes (Figure 2). Cosmogenic <sup>3</sup>He concentrations are calculated incrementally until present day. Starting elevations vary depending on models (see below) and finish at the current elevation for each site (site G = 1900 m and site D = 1690 m).

The following uplift histories have been modeled:

1. *No uplift (NU)*. This model assumes that there is no change in elevation from 13.4 Ma until present day.
2. *Early Miocene uplift (EMU)*. Uplift rates and times are constructed based on the uplift rates from the adjacent Pica region (Figure 1a) suggested by Victor et al. [2004] with the majority of the uplift occurring prior to 13.4 Ma. The paleoelevation model for both sites shows similar surface uplift rates and times of movement as faults within the Pica region [Victor et al., 2004].
3. *Linear Uplift (LU)*. This model assumes a linear rate of uplift from sea level at 27 Ma to present-day altitudes based on uplift rates from within the Coastal Cordillera [Delouis et al., 1998; Dunai et al., 2005].
4. *Late Miocene uplift (LMU)*. This model is based on rapid uplift during the late Miocene. The timing of elevation change was based on soil carbonate precipitation temperature, oxygen isotopes, fossil-leaf physiognomy, and paleosurface reconstruction presented in Hoke et al. [2007] and Garzzone et al. [2008]. Uplift rates were based on a conservative 800 m of uplift within the Longitudinal Valley in the late Miocene [Hoke et al., 2007]. Background uplift rate of 0.04 mm/yr of the Coastal Cordillera [Dunai et al., 2005] and minor movement along local faults based on Farías et al. [2005] were assumed to have operated from 13.4 Ma to the present day.

For each uplift history the three main in situ cosmogenic nuclide scaling models were used [*Lal*, 1991; *Dunai*, 2000; *Lifton* et al., 2014]. Palaeomagnetic data from northern Chile indicate that there has been no latitudinal translation of strata since the late Palaeozoic [Jesinkey et al., 1987; Hartley et al., 1988; Somoza and Tomlinson, 2002], so it is not necessary to calculate changes in production rate with latitude.

We have used the weighted mean of the cosmogenic <sup>3</sup>He production rate in olivine compiled by Goehring et al. [2010] and incorporated more recent measurements [Foeken et al., 2012; Blard et al., 2013]. The sea level high-latitude <sup>3</sup>He production rates used for the three scaling factors are 119.3 ± 3.0 atoms/g for *Lal* [1991],

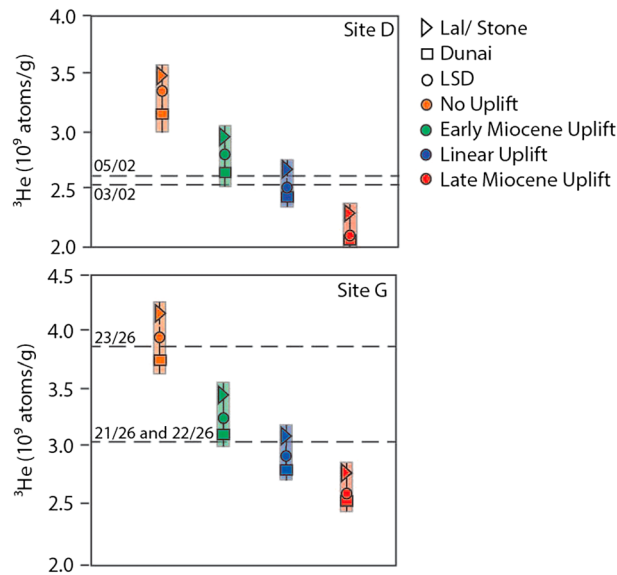


**Figure 3.** Concentration of cosmogenic  $^3\text{He}$  calculated for different uplift histories for two sites in Quebrada Aroma, northern Chile. Three scaling factor algorithms were considered; circle, *Lal* [1991], square; *Dunai* [2000], triangle; and *Lifton et al.* [2014], triangle. Symbols represent the  $^3\text{He}$  concentrations (atoms/g) for the four uplift scenarios (colors as per Figure 2). The horizontal dashed lines represent the He concentration of each sample.

samples using LAICPMS techniques (see supporting information). It ranges from 23–49 ppm and accounts for 6–12% of that produced by spallation (see supporting information).

### 5. Results

The cosmogenic  $^3\text{He}$  produced by spallation at each site, for each surface uplift scenario and scaling factors (Table 2), is plotted in Figure 3. It is important to stress that these modeled values are upper limits on the amount of cosmogenic He that has been produced as it assumes a maximum possible surface exposure age and does not take into account the effect of erosion, burial, or exhumation of the boulders during their residence on the surface. The spallation-produced cosmogenic  $^3\text{He}$  concentrations of each mineral sample are plotted as dashed lines on Figure 3. Correction for CTN-cosmogenic He has been made using measured Li in amphibole (Table S3 in the supporting information) and an upper limit of 5% for the pyroxenes which equates to 20 ppm Li [*Dunai et al.*, 2007; *Amidon and Farley*, 2012].

The rapid late Miocene uplift history predicts the lowest cosmogenic  $^3\text{He}$  concentrations ( $2.1$  to  $2.8 \times 10^9$  atoms/g) as the surfaces have spent the shortest time at high elevation. Cosmogenic  $^3\text{He}$  concentrations are predicted to be highest in samples that remained at the current elevation throughout their history ( $3.2$  to  $4.2 \times 10^9$  atoms/g). Uplift in the early Miocene gives concentrations in the range  $2.6$  to  $3.4 \times 10^9$  atoms/g, while linear uplift produces cosmogenic  $^3\text{He}$  concentrations of  $2.4$  to  $3.1 \times 10^9$  atoms/g. The scaling factors of *Dunai* [2000] systematically yield the lowest cosmogenic  $^3\text{He}$  concentrations, while those of *Lal* [1991] produce the highest.

The late Miocene uplift model generates maximum  $^3\text{He}$  concentrations that are lower than measured in all samples using all scaling factors (Figure 3). The samples contain  $0.2$ – $1.3 \times 10^9$  atoms  $^3\text{He/g}$  more  $^3\text{He}$  than late Miocene uplift predicts, depending on scaling scheme.

All samples except 23/26 have  $^3\text{He}$  concentrations that are predicted by a no uplift history or early Miocene uplift. The cosmogenic  $^3\text{He}$  concentration predicted by linear uplift using *Lal* [1991] scaling factors is higher than measured in the samples, except for sample 23/26. The  $^3\text{He}_{\text{cos}}$  concentration measured in boulder 23/26 overlaps that predicted for no uplift of the surface using the *Lal* [1991] or *Lifton et al.* [2014] scaling factors.

$121.2 \pm 3.2$  atoms/g for *Dunai* [2000], and  $114.6 \pm 3.0$  atoms/g for *Lifton et al.* [2014]. These were scaled for the composition of the analyzed minerals using the element production rates of *Masarik* [2002]. Production rates vary due to changes in the geomagnetic field strength and inclination through time, magnetic polar reversals, and differing flux of cosmic rays originating from the sun and cosmos. However, these effects are estimates to cancel out over timescales greater than  $<100$  kyr [*Dunai*, 2001].

The contribution of  $^3\text{He}$  produced by cosmogenic thermal neutrons (CTN) on  $^6\text{Li}$  cannot be ignored [*Dunai et al.*, 2007]. Lithium in andesites is relatively low ( $<20$  ppm), and due to mineral-melt partitioning coefficients it resides predominantly in the matrix, with pyroxenes displaying concentrations usually below 2 ppm. However, amphiboles typically have higher Li contents, and CTN-derived cosmogenic  $^3\text{He}$  can contribute up to 40% of total [*Amidon and Farley*, 2012]. Li was measured in the three amphibole

## 6. Discussion

### 6.1. Ruling Out Late Miocene Uplift

The principal aim of this work is to test whether or not the high concentrations of  $^3\text{He}_{\text{cos}}$  previously measured in alluvial boulders from Querada Aroma [Evenstar et al., 2009] can be accounted for by surface uplift in the late Miocene. The simple comparison with predicted  $^3\text{He}_{\text{cos}}$  concentrations clearly appears to exclude late Miocene uplift (Figure 3).

The boulders on the desert pavement may have undergone small degrees of erosion, suffered exhumation, and/or partial burial. All of these processes would decrease the cosmogenic He production rate and therefore yield lower concentrations compared to that produced by complete exposure. The effect of erosion is documented in the supporting information (Figure S3 in the supporting information). Using a low erosion rate of 1 cm/Myr shows how even a minor amount of erosion would greatly decrease the modeled concentrations. When comparing these modeled concentrations to measured  $^3\text{He}_{\text{cos}}$  in the alluvial boulders only assuming that no uplift had occurred over the last 13.4 Ma would be consistent with the data. As such erosional processes would lend support to an even earlier uplift model.

Preexposure of all the boulders prior to deposition on the PPS is the only process that could have increased the concentration of cosmogenic He. There are a number of reasons why a significant contribution of inheritance cannot account for the excess helium within the samples assuming late Miocene uplift.

Firstly, the similarity of the  $^3\text{He}$  concentration in four of the five samples, relative to elevation, is not typical of inheritance [Dunai et al., 2005; Nishiizumi et al., 2005; Kober et al., 2007; Fujioka et al., 2005; Blisniuk et al., 2012; Van der Wateren and Dunai, 2001]. It would require that each boulder has had a similar preexposure history and that each was deposited with the preexposed surface at the top of the boulder.

Secondly, the boulders on the PPS are located on the flat lying paleosurface, which is 60 km wide and slopes at an angle of  $1.5^\circ$  (Figure 1). The nearest significant large scarps for boulders to originate is over 20 km to the east. The boulders could only have moved in a large fluvial event originating within the Precordillera. Late Miocene uplift requires the isolation of the PPS at 10 Ma due to increased incision between the PPS and Precordillera. Therefore, the boulders on the PPS could only obtain significant preexposure from higher elevations prior to 10 Ma. At this time the elevation of the Precordillera and Western Cordillera was significantly lower than currently; the highest elevation is predicted to be  $\sim 3500$  m [Garzzone et al., 2008]. This makes accounting for the excess He within the samples highly unlikely. For instance, the excess  $^3\text{He}_{\text{cos}}$  in boulder 23/26 relative to that predicted by late Miocene uplift at 13.2 Ma ( $>1 \times 10^9$  atoms/g) is equivalent to  $\sim 13$  Myr exposure at sea level or 3 Myr exposure at the current altitude of Quebrada Aroma. The excess He requires preexposure for a minimum of  $\sim 1.5$  Myr at the highest possible elevation within the paleo-Andes prior to 13.4 Ma, assuming no surface erosion. The current erosion rate in the Western Cordillera is between 100 and 1000 cm/Myr at similar elevations [Kober et al., 2007]. Such high erosion rates are not conducive to preservation of enough cosmogenic He to account for the apparent excess.

In summary, it is unlikely that the PPS boulders have experienced significant preexposure; thus, the measured cosmogenic He reflects the surface uplift history. The late Miocene uplift model cannot produce enough cosmogenic  $^3\text{He}$  to account for the concentrations measured in the alluvial boulders from the PPS. The data do not constrain a single unique uplift history, but the data appear to require that the majority of the uplift occurred prior to the late Miocene.

### 6.2. Implications for Andean Uplift

Determining accurately the time of the onset of surface uplift throughout the Central Andes is essential for understanding the geodynamic mechanisms of plateau development at convergent continental margins and will help inform orogenic erosion, sedimentation, local and regional climates, and rainfall patterns [Barnes and Ehlers, 2009]. The results presented here suggest that the PPS obtained a substantial proportion of its elevation prior to 13.4 Ma. This is consistent with either an early phase of uplift in the early Miocene with relatively minor uplift after or relatively slow constant surface uplift rates for the western flank of the Andean Cordillera from 30 Ma or earlier.

This is independent of climate sensitive-altitude relationships and stands in marked contrast to previous studies that utilized oxygen isotopes [Garzzone et al., 2006], clumped C-O isotopes [Ghosh et al., 2006; Quade et al., 2007], and fluvial incision rate [Schildgen et al., 2007; Hoke et al., 2007; Thouret et al., 2007]

that suggest the majority of uplift occurred after 10 Ma. The results presented here fit the structural, surface incision, deformation/exhumation history, and timing of sedimentary deposition that indicate progressive surface uplift associated with crustal shortening from the late Eocene or earlier [Victor *et al.*, 2004; McQuarrie, 2002; Hoke and Lamb, 2007; Ehlers and Poulsen, 2009]. This is in contrast to the sudden, rapid uplift in the late Miocene that is associated with delamination of an overthickened orogenic crustal root [e.g., Garzzone *et al.*, 2008]. These observations suggest that large mountain chains can be created within ocean-continent subduction zone settings by progressive shortening and thickening of continental crust and without the need for large-scale mantle delamination.

#### Acknowledgments

This material is based upon work supported by NERC grant (NER/S/A/2003/11945) and BHP Billiton. Data used in this study are provided from *Evenstar et al.* [2009] and from modeling detailed in the supporting information. We are grateful to Philip G. Roxby, Steve Sparks, and Shasta Marrero for their help with preparation of the manuscript.

#### References

- Amidon, W. H., and K. A. Farley (2012), Cosmogenic  $^3\text{He}$  and  $^{21}\text{Ne}$  dating of biotite and hornblende, *Earth Planet. Sci. Lett.*, 313–314, 86–94, doi:10.1016/J.Epsl.2011.11.005.
- Barke, R., and S. Lamb (2006), Late Cenozoic uplift of the Eastern Cordillera, Bolivian Andes, *Earth Planet. Sci. Lett.*, 249(3–4), 350–367, doi:10.1016/J.Epsl.2006.07.012.
- Barnes, J. B., and T. A. Ehlers (2009), End member models for Andean Plateau uplift, *Earth Sci. Rev.*, 97(1–4), 105–132, doi:10.1016/J.Earscirev.2009.08.003.
- Blard, P. H., J. Lavé, F. Sylvestre, C. J. Placzek, C. Claude, V. Galy, T. Condom, and B. Tibari (2013), Cosmogenic  $^3\text{He}$  production rate in the high tropical Andes (3800 m, 20°S): Implications for the local last glacial maximum, *Earth Planet. Sci. Lett.*, 377–378, 260–275, doi:10.1016/j.epsl.2013.07.006.
- Blisniuk, K., M. Oskin, K. Fletcher, T. Rockwell, and W. Sharp (2012), Assessing the reliability of U-series and  $^{10}\text{Be}$  dating techniques on alluvial fans in the Anza Borrego Desert, California, *Quat. Geochronol.*, 13, 26–41, doi:10.1016/j.quageo.2012.08.004.
- Clift, P. D. (2010), Enhanced global continental erosion and exhumation driven by Oligo-Miocene climate change, *Geophys. Res. Lett.*, 37, L09402, doi:10.1029/2010GL043067.
- Delouis, B., H. Philip, L. Dorbath, and A. Cisternas (1998), Recent crustal deformation in the Antofagasta region (northern Chile) and the subduction process, *Geophys. J. Int.*, 132(2), 302–338, doi:10.1046/J.1365-246X.1998.00439.X.
- Dunai, T. J. (2000), Scaling factors for production rates of in situ produced cosmogenic nuclides: A critical reevaluation, *Earth Planet. Sci. Lett.*, 176(1), 157–169, doi:10.1016/S0012-821X(99)00310-6.
- Dunai, T. J. (2001), Influence of secular variation of the geomagnetic field on production rates of in situ produced cosmogenic nuclides, *Earth Planet. Sci. Lett.*, 193(1–2), 197–212, doi:10.1016/S0012-821X(01)00503-9.
- Dunai, T. J., G. A. G. Lopez, and J. Juez-Larre (2005), Oligocene-Miocene age of aridity in the Atacama Desert revealed by exposure dating of erosion-sensitive landforms, *Geology*, 33(4), 321–324, doi:10.1130/G21184.1.
- Dunai, T. J., F. M. Stuart, R. Pik, P. Burnard, and E. Gayer (2007), Production of  $^3\text{He}$  in crustal rocks by cosmogenic thermal neutrons, *Earth Planet. Sci. Lett.*, 258(1–2), 228–236, doi:10.1016/J.Epsl.2007.03.031.
- Ehlers, T. A., and C. J. Poulsen (2009), Influence of Andean uplift on climate and paleoaltimetry estimates, *Earth Planet. Sci. Lett.*, 281(3–4), 238–248, doi:10.1016/j.epsl.2009.02.026.
- Evenstar, L. A., A. J. Hartley, F. M. Stuart, A. E. Mather, C. M. Rice, and G. Chong (2009), Multiphase development of the Atacama Planation Surface recorded by cosmogenic  $^3\text{He}$  exposure ages: Implications for uplift and Cenozoic climate change in western South America, *Geology*, 37(7), 658–658, doi:10.1130/G25437A.1.
- Fariás, M., R. Charrier, D. Comte, J. Martinod, and G. Hérail (2005), Late Cenozoic deformation and uplift of the western flank of the Altiplano: Evidence from the depositional, tectonic, and geomorphologic evolution and shallow seismic activity (northern Chile at 19°30'S), *Tectonics*, 24, TC4001, doi:10.1029/2004TC001667.
- Foeken, J. P. T., F. M. Stuart, and D. F. Mark (2012), Long-term low latitude cosmogenic  $^3\text{He}$  production rate determined from a 126 ka basalt from Fogo, Cape Verdes, *Earth Planet. Sci. Lett.*, 359, 14–25, doi:10.1016/J.Epsl.2012.10.005.
- Fujioka, T., J. Chappell, M. Honda, I. Yatsevich, K. Fifield, and D. Fabel (2005), Global cooling initiated stony deserts in central Australia 2–4 Ma, dated by cosmogenic  $^{21}\text{Ne}$ - $^{10}\text{Be}$ , *Geology*, 33(12), 993–996, doi:10.1130/g21746.1.
- Garzzone, C. N., P. Molnar, J. C. Libarkin, and B. J. MacFadden (2006), Rapid late Miocene rise of the Bolivian Altiplano: Evidence for removal of mantle lithosphere, *Earth Planet. Sci. Lett.*, 241(3–4), 543–556, doi:10.1016/j.epsl.2005.11.026.
- Garzzone, C. N., G. D. Hoke, J. C. Libarkin, S. Withers, B. MacFadden, J. Eiler, P. Ghosh, and A. Mulch (2008), Rise of the Andes, *Science*, 320(5881), 1304–1307, doi:10.1126/science.1148615.
- Ghosh, P., C. N. Garzzone, and J. M. Eiler (2006), Rapid uplift of the Altiplano revealed through  $^{13}\text{C}$ - $^{18}\text{O}$  bonds in paleosol carbonates, *Science*, 311(5760), 511–515, doi:10.1126/Science.1119365.
- Goehring, B. M., M. D. Kurz, G. Balco, J. M. Schaefer, J. Licciardi, and N. Lifton (2010), A reevaluation of in situ cosmogenic  $^3\text{He}$  production rates, *Quat. Geochronol.*, 5(4), 410–418, doi:10.1016/J.Quageo.2010.03.001.
- Hartley, A. J. (2003), Andean uplift and climate change, *J. Geol. Soc. London*, 160, 7–10, doi:10.1144/0016-764902-083.
- Hartley, A. J., P. Turner, G. D. Williams, and S. Flint (1988), Palaeomagnetism of the Cordillera de la Costa, northern Chile: Evidence for local forearc rotation, *Earth Planet. Sci. Lett.*, 89(3–4), 375–386, doi:10.1016/0012-821X(88)90124-0.
- Hartley, A. J., G. May, G. Chong, P. Turner, S. J. Kape, and E. J. Jolley (2000), Development of a continental forearc: A Cenozoic example from the Central Andes, northern Chile, *Geology*, 28(4), 331–334, doi:10.1130/0091-7613(2000)28<331:Doacfa>2.0.Co;2.
- Hartley, A. J., T. Sempere, and G. Wörner (2007), A comment on “Rapid late Miocene rise of the Bolivian Altiplano: Evidence for removal of mantle lithosphere” by C.N. Garzzone *et al.* [Earth Planet. Sci. Lett. 241 (2006) 543–556], *Earth Planet. Sci. Lett.*, 259(3–4), 625–629, doi:10.1016/J.Epsl.2007.04.012.
- Hoke, G. D., and C. N. Garzzone (2008), Paleosurfaces, paleoelevation, and the mechanisms for the late Miocene topographic development of the Altiplano plateau, *Earth Planet. Sci. Lett.*, 271(1–4), 192–201, doi:10.1016/J.Epsl.2008.04.008.
- Hoke, G. D., B. L. Isacks, T. E. Jordan, N. Blanco, A. J. Tomlinson, and J. Ramezani (2007), Geomorphic evidence for post-10 Ma uplift of the western flank of the central Andes 18°30'–22°S, *Tectonics*, 26, TC5021, doi:10.1029/2006TC002082.
- Hoke, L., and S. Lamb (2007), Cenozoic behind-arc volcanism in the Bolivian Andes, South America: Implications for mantle melt generation and lithospheric structure, *J. Geol. Soc. London*, 164, 795–814, doi:10.1144/0016-76492006-092.

- Jeffery, M. L., T. A. Ehlers, B. J. Yanites, and C. J. Poulsen (2013), Quantifying the role of paleoclimate and Andean Plateau uplift on river incision, *J. Geophys. Res. Earth Surf.*, *118*, 852–871, doi:10.1002/jgrf.20055.
- Jesinkey, C., R. D. Forsythe, C. Mpodozis, and J. Davidson (1987), Concordant late Paleozoic paleomagnetizations from the Atacama Desert: Implications for tectonic models of the Chilean Andes, *Earth Planet. Sci. Lett.*, *85*(4), 461–472, doi:10.1016/0012-821X(87)90141-5.
- Kober, F., F. Schlunegger, G. Zeilinger, and H. Schneider (2006), Surface uplift and climate change: The geomorphic evolution of the Western Escarpment of the Andes of northern Chile between the Miocene and present, *Geol. Soc. Am. Bull.*, *398*, 75–86, doi:10.1130/2006.2398(05).
- Kober, F., S. Ivy-Ochs, F. Schlunegger, H. Baur, P. W. Kubik, and R. Wieler (2007), Denudation rates and a topography-driven rainfall threshold in northern Chile: Multiple cosmogenic nuclide data and sediment yield budgets, *Geomorphology*, *83*(1–2), 97–120, doi:10.1016/j.geomorph.2006.06.029.
- Lal, D. (1991), Cosmic ray labeling of erosion surfaces: In situ nuclide production rates and erosion models, *Earth Planet. Sci. Lett.*, *104*(2–4), 424–439, doi:10.1016/0012-821X(91)90220-C.
- Lifton, N., T. Sato, and T. J. Dunai (2014), Scaling in situ cosmogenic nuclide production rates using analytical approximations to atmospheric cosmic-ray fluxes, *Earth Planet. Sci. Lett.*, *386*, 149–160, doi:10.1016/j.epsl.2013.10.052.
- Margerison, H. R., W. M. Phillips, F. M. Stuart, and D. E. Sugden (2005), Cosmogenic <sup>3</sup>He concentrations in ancient flood deposits from the Coombs Hills, northern Dry Valleys, East Antarctica: Interpreting exposure ages and erosion rates, *Earth Planet. Sci. Lett.*, *230*, 163–175, doi:10.1016/j.epsl.2004.11.007.
- Masarik, J. (2002), Numerical simulation of in-situ production of cosmogenic nuclides, *Geochim. Cosmochim. Acta*, *66*(15A), A491–A491, doi:10.1016/j.nimb.2007.03.003.
- McQuarrie, N. (2002), The kinematic history of the central Andean fold-thrust belt, Bolivia: Implications for building a high plateau, *Geol. Soc. Am. Bull.*, *114*(8), 950–963, doi:10.1130/0016-7606(2002)114<0950:Tkhoc>2.0.Co;2.
- Molnar, P., and C. N. Garzione (2007), Bounds on the viscosity coefficient of continental lithosphere from removal of mantle lithosphere beneath the Altiplano and Eastern Cordillera, *Tectonics*, *26*, TC2013, doi:10.1029/2006TC001964.
- Muñoz, N., and P. Sepúlveda (1992), Estructuras compresivas convergencia al Oeste en el borde oriental de la Depresión Central (19°15' lat. Sur), *Rev. Geol. Chile*, *19*, 214–247, doi:10.5027/andgeoV19n2-a07.
- Nishiizumi, K., M. W. Caffee, R. C. Finkel, G. Brimhall, and T. Mote (2005), Remnants of a fossil alluvial fan landscape of Miocene age in the Atacama Desert of northern Chile using cosmogenic nuclide exposure age dating, *Earth Planet. Sci. Lett.*, *237*(3–4), 499–507, doi:10.1016/j.epsl.2005.05.032.
- Pinto, L., G. Hérail, and R. Charrier (2004), Syntectonic sedimentation associated with Neogene structures in the Precordillera of Moquella Zone, Tarapacá (19°15'S, northern Chile), *Rev. Geol. Chile*, *31*, 19–44, doi:10.4067/S0716-02082004000100002.
- Pinto, L., G. Hérail, F. Fontan, and P. De Parseval (2007), Neogene erosion and uplift of the western edge of the Andean plateau as determined by detrital heavy mineral analysis, *Sediment. Geol.*, *195*, 217–237, doi:10.1016/j.sedgeo.2006.08.001.
- Quade, J., C. Garzione, and J. Eiler (2007), Paleoelevation reconstruction using pedogenic carbonates, *Rev. Mineral. Geochem.*, *66*(1), 53–87, doi:10.2138/rmg.2007.66.3.
- Riihimäki, C. A., and J. C. Libarkin (2007), Terrestrial cosmogenic nuclides as paleoaltimetric proxies, *Rev. Mineral. Geochem.*, *66*, 269–278, doi:10.2138/Rmg.2007.66.11.
- Schildgen, T. F., K. V. Hodges, K. X. Whipple, P. W. Reiners, and M. S. Pringle (2007), Uplift of the western margin of the Andean plateau revealed from canyon incision history, southern Peru, *Geology*, *35*(6), 523, doi:10.1130/g23532a.1.
- Somoza, R., and A. Tomlinson (2002), Paleomagnetism in the Precordillera of northern Chile (22°30'S): Implications for the history of tectonic rotations in the Central Andes, *Earth Planet. Sci. Lett.*, *194*(3–4), 369–381, doi:10.1016/S0012-821X(01)00548-9.
- Thouret, J. C., G. Wörner, Y. Gunnell, B. Singer, X. Zhang, and T. Souriot (2007), Geochronologic and stratigraphic constraints on canyon incision and Miocene uplift of the Central Andes in Peru, *Earth Planet. Sci. Lett.*, *263*(3–4), 151–166, doi:10.1016/j.epsl.2007.07.023.
- Van der Wateren, F. M., and T. J. Dunai (2001), Late Neogene passive margin denudation history—cosmogenic isotope measurements from the central Namib desert, *Global Planet. Change*, *30*(3–4), 271–307, doi:10.1016/S0921-8181(01)00104-7.
- Victor, P., O. Oncken, and J. Glodny (2004), Uplift of the western Altiplano plateau: Evidence from the Precordillera between 20° and 21°S (northern Chile), *Tectonics*, *23*, TC4004, doi:10.1029/2003TC001519.
- von Rotz, R., F. Schlunegger, F. Heller, and I. Villa (2005), Assessing the age of relief growth in the Andes of northern Chile: Magneto-polarity chronologies from Neogene continental sections, *Terra Nova*, *17*, 462–471, doi:10.1111/j.1365-3121.2005.00634.x.
- Wörner, G., D. Uhlig, I. Kohler, and H. Seyfried (2002), Evolution of the West Andean Escarpment at 18°S (N. Chile) during the last 25 Ma: Uplift, erosion and collapse through time, *Tectonophysics*, *345*(1–4), 183–198, doi:10.1016/S0040-1951(01)00212-8.

## Erratum

In the originally published version of this article, the name of co-author Brian Tattich was misspelled. The error has since been corrected, and this version may be considered the authoritative version of record.

In the author line, “Brain Tattich” has been corrected to read “Brian Tattich.”